Nickel(II) Metal-Organic Frameworks with N,N'-di(4-pyridyl)-1,4,5,8-naphthalenetetracarboxydiimide Ligands: Influence of Secondary Building Unit Geometry on Dimensionality and Framework Dimensions.

*Constance R. Pfeiffer, Naomi H. Biggins, William Lewis, and Neil R. Champness**

University of Nottingham, School of Chemistry, Nottingham, NG7 2RD, England.

Email: Neil.Champness@nottingham.ac.uk

Keywords: Metal-organic frameworks, *N,N'*-di(4-pyridyl)-1,4,5,8-naphthalenetetracarboxydiimide, nickel (II) frameworks, pillared frameworks.

Abstract

When $Ni(NO_3)_2 \cdot 6H_2O$ and *N,N'*-di(4-pyridyl)-1,4,5,8-naphthalenetetracarboxydiimide (DPNDI) are reacted, a one-dimensional coordination polymer (**1**) is formed. However, reaction with either terephthalic acid (**2**) or 2,6-naphthalenedicarboxylic acid (**3**) affords two-dimensional, pillared metal-organic frameworks. **2** and **3** containing rectangular voids of different dimensions which are dictated by the carboxylate ligand and the arrangement of the $[M(\kappa^2\text{-}O_2NO)]_2(\mu^2\text{-}O_2CR)_2]$ secondary building unit (SBU) that forms the nodes of the framework. The role of SBU geometry, intermolecular face-to-face π–π and lone pair–π interactions involving the DPNDI ligands are discussed.

Introduction

Metal-organic frameworks, or MOFs, have developed rapidly as a field of research. Evolving from the original concepts of the building-block approach, the field has reached a position where a large variety of framework materials are being applied to a myriad of applications.[1,2] Thus, in addition to studies that exploit the porosity of MOFs for gas storage[3] developments have been made in a

number of other areas including biological applications,[4-6] conductivity,[7] crystalline sponges,[8] and as matrices for probing chemical reactions.[9] As a result of the modular, building-block approach it is possible to incorporate specific components into the framework that impart specific properties on the resulting material. Thus, ligands that possess such properties can be attractive to target designed MOFs. An example of a family of interesting ligands is those that contain naphthalene diimide (NDI) cores. NDIs are highly functionalised, π-conjugated molecules that can be tailored to various applications. The core of the NDI is strongly electron deficient, and thus can interact readily with electron-rich species.[10] Additionally, NDIs are both redox active and fluorescent.[10] Due to the flexibility in functionality and their potential redox reactivity, it can be advantageous to use functionalised NDIs as linkers in metal organic frameworks (MOFs).[11] One such NDI-containing ligand that has been employed in the construction of MOFs is *N,N'*-di(4-pyridyl)-1,4,5,8-naphthalenetetracarboxydiimide (DPNDI).[12-32]

One of the most attractive features of MOFs is the ability to prepare materials that exhibit permanent microporosity.[1-3] One approach that has been successfully employed to create such systems are mixed-ligand frameworks where tunable cavities are obtained using a pillaring approach.[12-16,34] Typically pillaring creates three-dimensional frameworks by using rigid linkers (pillars) to connect two-dimensional layers, but the same approach can be used to create two-dimensional structures depending on the arrangement of the metal-based secondary building units (SBUs). By employing two different linkers greater flexibility, structural diversity, and control over porosity can be achieved. For example, Hupp *et al* have used *N,N'*-di(4-pyridyl)-1,4,5,8-naphthalenetetracarboxydiimide (DPNDI) in combination with different length dicarboxylic acid linkers to create zinc pillared MOFs with tunable pore and channel dimensions.[35]

However, despite the many attractive features of MOFs and the successes that have been achieved in the area, there are still significant synthetic challenges in the delivery of target MOF structures. Herein we report a structural study of a Ni(II)-DPNDI coordination polymer[36] and two MOFs in combination with pillaring dicarboxylate linkers, the first examples of such nickel-based MOFs. All three MOF systems use DPNDI and Ni(II) to create one-dimensional polymers and in the case of the two MOFs, terephthalate (BDC^{2-}) in **2** and 2,6-naphthalenedicarboxylate (NDC^{2-}) in **3** act as pillars (Figure 1). In the case of **2** and **3**, differences in the arrangement of the secondary building unit (SBU), as result of nickel-nitrate coordination, results in lower dimensionality (2D vs. 3D) and smaller pore size in comparison to analogous Zn(II) frameworks.

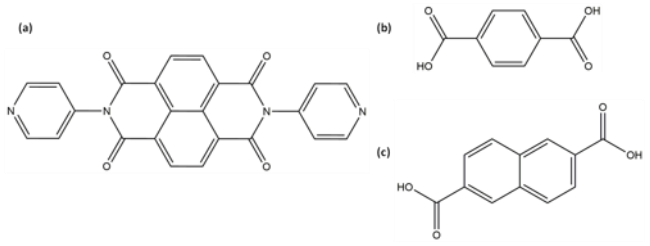

Figure 1. Ligands employed in this study. (a) N,N'-di(4-pyridyl)-1,4,5,8-naphthalenetetracarboxydiimide (DPNDI) (b) terephthalic acid (BDC), and (c) 2,6-napthalenedicarboxylic acid (NDC).

Results and discussion

Single crystals of compound **1** were grown under solvothermal conditions, reacting $Ni(NO_3)_2 \cdot 6H_2O$ with DPNDI in DMF. The single crystal X-ray structure reveals that **1** is a one-dimensional coordination polymer that is composed of alternating Ni(II) cations and bridging DPNDI ligands (Figure 2).

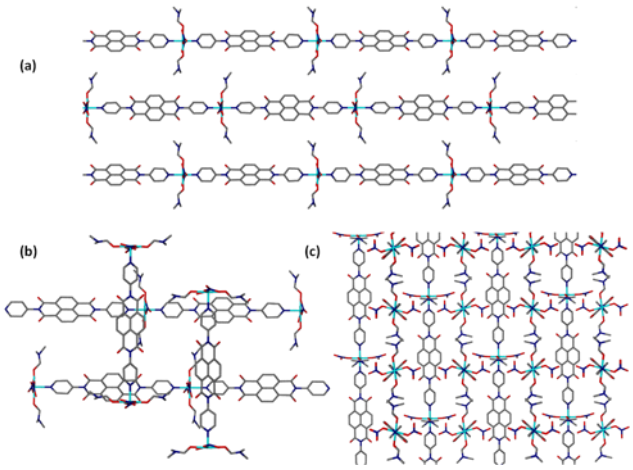

Figure 2. (a) Orientation of the 1D chains in **1** on the *ab*-axis. Adjacent chains (in opposite orientation) are removed for clarity. (b) Both orientations of the chains along the *ab*-axis. (c) Packing along the *ac*-axis. All hydrogen atoms have been removed for clarity and the highest occupancy disorder component is shown. Carbon atoms = grey, oxygen atoms = red atoms, nitrogen atoms = dark blue, and nickel atoms = light blue.

The Ni(II) centre is octahedrally coordinated to two DMF molecules, two monodentate, η^1, nitrate anions, and two DPNDI ligands. Each pair of ligand type are arranged in a *trans* arrangement (Figure 3). See Supporting Information for bond lengths and angles associated with the Ni(II)

cation. The compound crystallises in the tetragonal space group $I\bar{4}2d$ such that adjacent chains alternate in perpendicular directions throughout the structure; if one layer has the DPNDI ligand oriented horizontally, then the adjacent chains have the DPNDI ligand oriented vertically. The DPNDI ligands are not arranged to allow for face-to-face or edge-to-face contacts for π–π interactions; however, lone pair–π interactions are observed (Figure 4) through interactions of the lone pair of elections of a nitrate oxygen atom and the electron-poor, π–acidic cores of the DPNDI ligands. These interactions form a pseudo bridge between the chains (Figure 4). Previous studies with DPNDI/metal coordination polymers by Lin *et. al.*[37] have shown similar lone pair–π interactions in a series of six one-dimensional metal coordination polymers that are structurally related to **1**, varying in the transition metal employed and the solvents/ligands coordinated to that metal centre. A comparison between the lone pair–π interactions in this series of compounds and **1** can be found in Table 1.

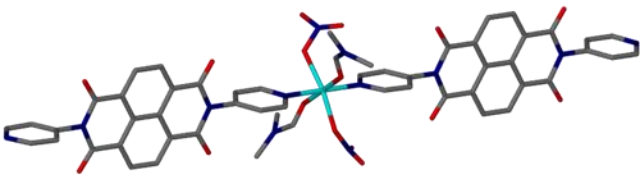

Figure 3. Coordination of DMF and nitrate ligands around the Ni(II) centre of **1**. All hydrogen atoms and disordered ligands have been removed for clarity. Carbon atoms = grey, oxygen atoms = red, nitrogen atoms = dark blue, and nickel atoms = light blue.

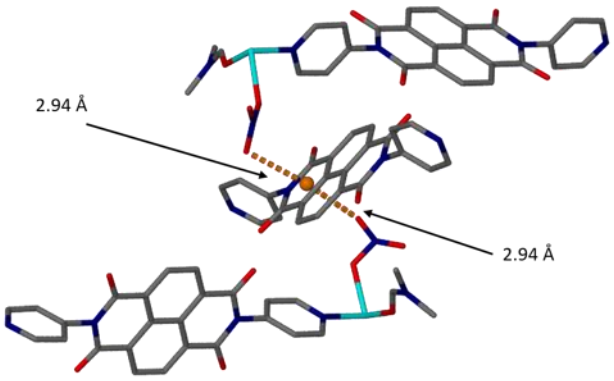

Figure 4. Lone pair–π interactions (dashed orange bonds) observed in **1** between the lone pairs of the oxygen atoms of the nitrate groups and the core of an adjacent DPNDI. Orange sphere

represents the centroid of the aromatic rings. All hydrogen atoms have been removed for clarity. Carbon atoms = grey, oxygen atoms = red, nitrogen atoms = dark blue, and nickel atoms = light blue.

Table 1. Comparison of lone pair–π interactions for structurally-related one-dimensional coordination polymers containing DPNDI.

Compound	**Auxiliary Ligand (L)**	**Lone pair–π length (Å)**
1	DMF	2.94
DPNDI[37]	DMF	3.14
$[Co(DPNDI)(NO_3)_2(L)]_\infty$ [37]	H_2O	3.15
$[Co(DPNDI)(NO_3)_2(L)_2]_\infty$ [37]	NMP	2.81
$[Cu(DPNDI)(NO_3)_2(L)]_\infty$ [37]	H_2O	3.03
$[Cu(DPNDI)(NO_3)_2(L)_2]_\infty$ [37]	NMP	2.91
$[Zn(DPNDI)(NO_3)_2(L)]_\infty$ [37]	H_2O	3.14
$[Zn(DPNDI)(NO_3)_2(L)_2]_\infty$ [37]	NMP	2.81

NMP = N-methylpyrrolidone.

Single crystals of **2** and **3** were grown under solvothermal conditions, reacting $Ni(NO_3)_2{\cdot}6H_2O$ with DPNDI and the appropriate dicarboxylate, terephthalic acid (**2**) and 2,6-naphthalene dicarboxylic acid (**3**), in DMF. The single crystal X-ray structures reveal two related two-dimensional pillared MOF structures. In both MOFs the Ni(II) cations are octahedrally coordinated to two DPNDI ligands in a *trans*-arrangement, two carboxylate linkers, that bridge to a second Ni(II) centre, and one k^2-nitrate ligand (Figure 5). For bonds lengths and angles between the Ni(II) centre and coordinated ligands see SI. Each of the metal cations is bridged through two μ^2-carboxylates leading to a dinuclear unit which is then capped by an k^2-nitrate ligand leading to a $[M(k^2\text{-}O_2NO)]_2(\mu^2\text{-}O_2CR)_2]$ SBU. These dinuclear SBUs are coordinated by four DPNDI ligands leading to the formation of pairs of bridged, one-dimensional chains of alternating Ni(II) cations and DPNDI ligands. These pairs of chains can also be viewed as ladders where alternating $(Ni\text{-}DPNDI)_\infty$ chains, similar to those observed in **1**, are bridged by μ^2-carboxylate donors which act as the rungs of the ladder.

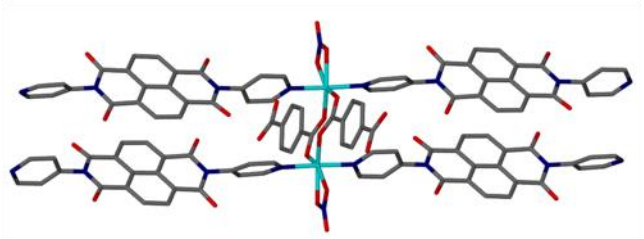

Figure 5. Coordination of terephthalate, nitrate, and DPNDI ligands around the Ni(II) centre of **2**. An analogous arrangement is observed in **3**. All hydrogen atoms have been removed for clarity.

Carbon atoms = grey, oxygen atoms = red, nitrogen atoms = dark blue, and nickel atoms = light blue.

Interestingly, between the adjacent DPNDI ligands of the ladders in **2** and **3**, face-to-face π–π interactions (**2**: 3.56 Å, 1.06 Å shift; **3**: 3.55 Å, 1.15 Å shift) are observed and, between adjacent two-dimensional sheets, lone pair-π interactions between the core of the DPNDI ligands and the lone pair of the oxygens of a nitrate ligand (**2**: 3.257 Å; **3**: 3.146 Å) (Figure 6). It is interesting to speculate whether these intermolecular interactions lead to the adoption of a more densely packed structure which restricts the formation of solvent-accessible voids.

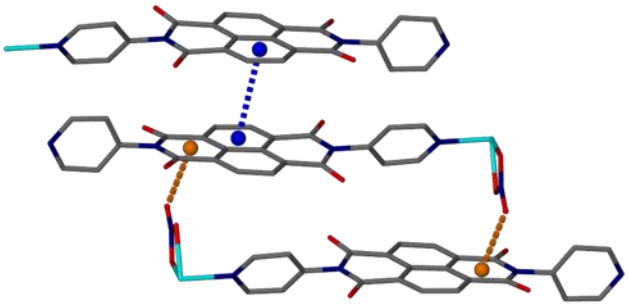

Figure 6. The lone pair–π interactions (dashed orange bonds) and π–π interactions (dashed blue bonds) in **2**. All hydrogen atoms and solvent atoms have been removed for clarity. Blue and orange spheres represent centroids of respective aromatic rings. Carbon atoms = grey, oxygen atoms = red, nitrogen atoms = dark blue, and nickel atoms = light blue.

Inspection of the extended structures of **2** and **3** shows that the DPNDI-Ni(II) ladders are connected through dicarboxylate pillars (Figures 7, 8) leading to two-dimensional sheets that contain rectangular voids. The dimensions of these channels are determined to be *ca*. 5.16 x 19.60 $Å^2$ (**2**) or 8.54 x 19.59 $Å^2$ (**3**). Using PLATON[38] the solvent accessible void volume was calculated in both **2** and **3** and was found to be 663 $Å^3$ (38%) and 889 $Å^3$ (44%) per unit cell respectively. In terms of solvent accessible void per formula unit, which is also per DPNDI, the void is smaller 331.5 $Å^3$ (**2**) and 444.5 $Å^3$ (**3**) (Table 2). Kitagawa *et al* have reported a related framework to **2** but with Zn(II) replacing Ni(II).[30] The only difference between the two structures is that the Zn(II) centre is coordinated to a single DPNDI ligand, in a *trans* arrangement as with **1**-**3**, but also to four separate carboxylate donors such that a classic paddlewheel $Zn_2(\mu^2\text{-}O_2CR)_4$ SBU is observed leading to a doubly interpenetrated three-dimensional MOF, $[Zn_2(BDC)_2DPNDI]_\infty$ (Figure 9). The channels in the Zn(II) structure have dimensions of approximately 6.11 x 18.71 $Å^2$, similar to those

observed in **2** and **3**, and in terms of solvent accessible void volume per formula unit (i.e. per DPNDI ligand) of 571 Å^3 is observed, similar to that observed for **2** and **3** (Table 2). Hupp *et al*[35] have similarly reported a structure related to that of Kitagawa[30] containing the same paddlewheel $Zn_2(\mu^2\text{-}O_2CR)_4$ SBU leading to two-dimensional sheets which are pillared by DPNDI, but using 2,6-naphthalene dicarboxylate as the anionic ligand, $[Zn_2(NDC)_2DPNDI]_\infty$, as used in **3**. In the case of $[Zn_2(NDC)_2DPNDI]_\infty$ the voids have dimensions of approximately 6.52 x 17.01 Å, smaller than those observed in **3**, but resulting in a larger guest-accessible void of 1005.8 Å^3 (54%) per formula unit (Table 2). The three-dimensional nature of $[Zn_2(NDC)_2DPNDI]_\infty$ accounts for the larger accessible void in comparison to **2** and **3** and is larger per formula unit than that observed for $[Zn_2(BDC)_2DPNDI]_\infty$ due to double interpenetration in the latter case.

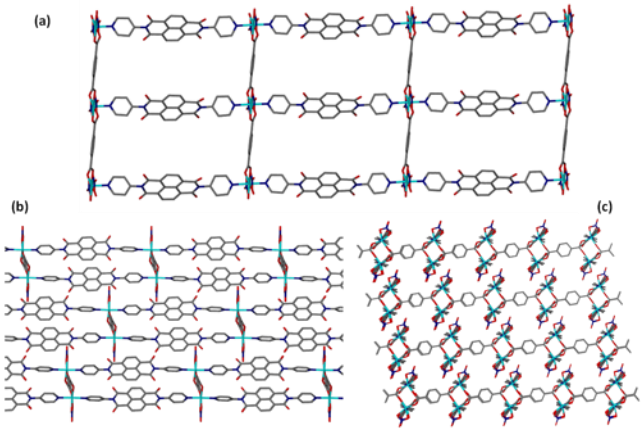

Figure 7. (a) Orientation of **2** on the *ac*-axis, (b) *bc*-axis, and (c) *ab*-axis. All hydrogen atoms and solvent molecules have been removed for clarity. Carbon atoms = grey, oxygen atoms = red, nitrogen atoms = dark blue, and nickel atoms = light blue.

In order to assess whether **2** and **3**, in particular, would be stable with respect to guest removal the compounds were investigated by powder X-ray diffraction (PXRD) and were found to be sensitive to even gentle drying processes (see supporting information for experimental and calculated patterns). In the case of compound **1** the drying process resulted in almost total loss of crystallinity with no evidence of the retention of the structure observed in the single crystal studies. PXRD diffractograms recorded for compound **3** and to a lesser extent compound **2** show significant broadening of the diffraction peaks indicating a loss of crystallinity upon drying of samples. Thus no further attempts were made to investigate the porosity of the three materials.

Conclusion

It is apparent that the framework arrangement adopted in **2** and **3** leads to a significantly smaller solvent-accessible void in comparison to related Zn(II)-DPNDI frameworks.[30,35] There are clear differences between the structures reported here and the related Zn(II) structures. In **2** and **3**, rather than forming a conventional paddlewheel, $M_2(\mu^2\text{-}O_2CR)_4$, SBU the presence of coordinated η^2-nitrate ligands alters the overall arrangement of the SBU, now $[M(\kappa^2\text{-}O_2NO)]_2(\mu^2\text{-}O_2CR)_2]$, such that each metal is bound by two DPNDI ligands rather than one each in the case of the Zn(II)-DPNDI frameworks. This facilitates the adoption of face-to-face π–π interactions in **2** and **3**, and the formation of ladder structures. Such arrangements are not seen in $[Zn_2(BDC)_2DPNDI]_\infty$ or $[Zn_2(NDC)_2DPNDI]_\infty$. The resulting two-dimensional frameworks observed in **2** and **3**, contrasting with the three-dimensional structures of the related Zn(II) structures, also allows close approach of adjacent frameworks enabling lone pair-π interactions between the nitrate ligands on one sheet and DPNDI ligands on adjacent sheets. Thus, the change in SBU observed in the Ni(II) structures reported here not only leads to a lower dimensionality of the overall framework (2D vs. 3D) but also allows the adoption of intermolecular interactions involving the DPNDI ligands which restrict solvent accessible voids in the framework structures. The role of the SBU structure and its subsequent effect on both framework dimensionality and upon the adoption of intermolecular interactions and closer packing are clearly important matters in the construction and design of the frameworks based using DPNDI and we believe that the current study provides valuable insight into the preparation of MOFs using this important class of ligand.

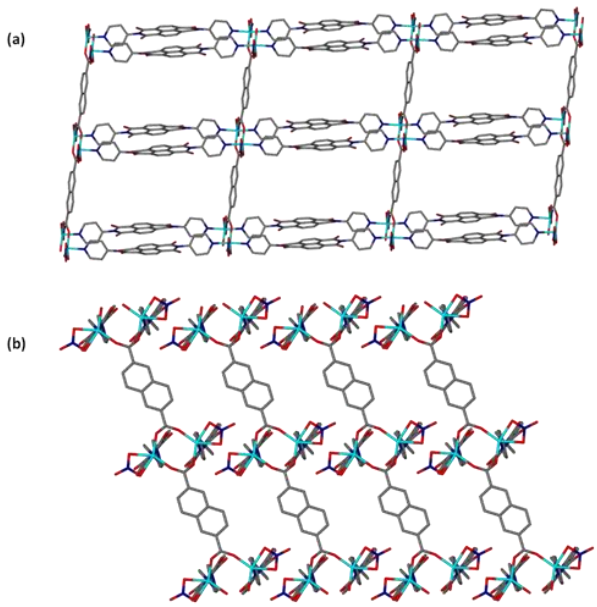

Figure 8. (a) Orientation of **3** along the *bc*-axis and (b) *ab*-axis. All hydrogen atoms and solvent molecules have been removed for clarity. Carbon atoms = grey, oxygen atoms = red, nitrogen atoms = dark blue, and nickel atoms = light blue.

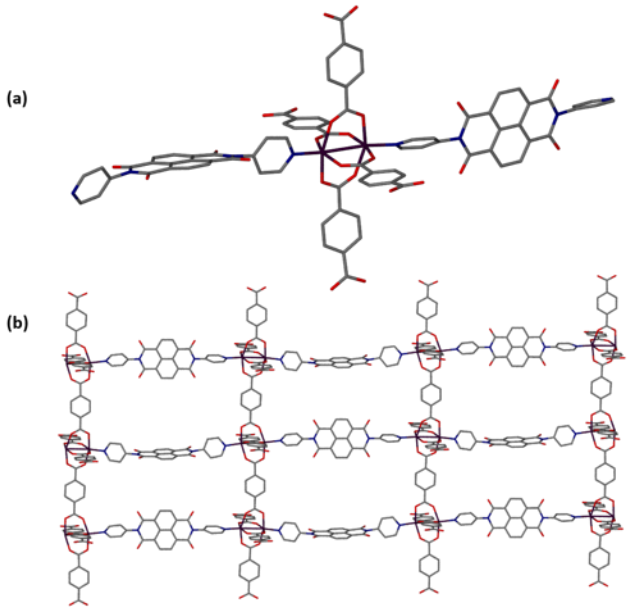

Figure 9. (a) Coordination of terephthalate, nitrate, and DPNDI ligands around the Zn(II) centre of Kitagawa[29] MOF. (b) Orientation along the *ac*-axis All hydrogen atoms have been removed for clarity. Carbon atoms = grey, oxygen atoms = red, nitrogen atoms = dark blue, and nickel atoms = purple.

Table 2. Solvent accessible void volumes in DPNDI MOFs

MOF	Metal centre	Number of DMF molecules	V_{free}(Å^3)/Z[b]	Volume (%)	Dimensions (Å^2)
2	Ni(II)	3[a]	331.5	38	5.16 x 19.60
3	Ni(II)	6[a]	444.5	44	8.54 x 19.59
$[Zn_2(BDC)_2DPNDI]_\infty$[30]	Zn(II)	4	571	43	6.11 x 18.71
$[Zn_2(NDC)_2DPNDI]_\infty$[35]	Zn(II)	6.51 [a]	1005.8	54	6.52 x 17.01

[a] Estimated from the excluded electrons per unit cell calculated after performing SQUEEZE. [b] Also corresponds to V_{free}(Å^3) per DPNDI ligand.

Experimental

All materials were obtained commercially and used without further purification. DPNDI was synthesised using a method previously described by Lu *et al*.[39] Single-crystal X-ray diffraction experiments were performed on an Oxford Diffraction SuperNova CCD area detector diffractometer operating at 120 K using mirror-monochromated Cu *K*α radiation (λ = 1.5418 Å). Gaussian grid face-indexed absorption correction with a beam profile correction (Crysalis Pro) was applied.[40] The structures were solved by direct methods using SHELXT[41] and refined by full-matrix least squares on F^2 using SHELXL.

1 was synthesised by combining 30 mg $Ni(NO_3)_2{\cdot}6H_2O$, 11 mg DPNDI, and 2 mL *N*,*N*'-dimethylformamide (DMF) in a sealed scintillation vial. The mixture was heated in an oven at 100°C for one day and yielded colourless, block-shaped crystals. (yield, 38 mg, 57%). FT-IR (ATR, cm^{-1}): 3149w, 3076w, 1712m, 1665m, 1580s, 1427m, 1376m, 1343s, 1247m, 1194m, 1064w, 1043w, 1028w, 986w, 822m, 766m, 659w.

Crystal data for **1**: $C_{90}H_{174}N_{28}NiO_{36}$. Tetragonal, space group $I\bar{4}2d$, a = b = 19.5137(6), c = 22.1533(16) Å, V = 8435.7(8) Å^3, Z = 8, D_{calc} = 3.596 g cm^{-3}, μ = 2.727 mm^{-1}, F(000) = 9808. A total of 9272 reflections were collected, of which 3635 were unique, with R_{int} = 0. 0545. Final R_1 (wR_2) = 0. 074 (0.204) with GOF = 1.08. Flack parameter = 0.17(9).

2 was synthesised by combining 30 mg $Ni(NO_3)_2{\cdot}6H_2O$, 9 mg terephthalic acid (BDC), 11 mg DPNDI, and 2 mL of DMF in a sealed scintillation vial. The mixture was heated in an oven at 130°C for one day and yielded colourless, plate-shaped crystals. (yield, 35 mg, 55%). FT-IR (ATR, cm^{-1}): 3084w, 2926w, 1716m, 1653s, 1577s, 1498, 1438m, 1382s, 1345s, 1247s, 1213m, 1192m,

1148m, 1098m, 1063m, 1018m, 983m, 869m, 856m, 821m, 765m, 749s, 716m, 664s, 639m, 578m, 532s, 422m.

Crystal data for **2**: $C_{37}H_{35}N_8NiO_{12}$. Triclinic, space group *P*-1, a = 9.8571(6), b = 11.2573(7), c = 16.1205(8) Å, α = 89.642(4), β = 83.978(5), γ =82.956(5)°, V = 1765.46(18) Å^3, Z = 2, D_{calc} = 1.585 g cm^{-3}, μ = 1.489 mm^{-1}, F(000) = 874. A total of 14637 reflections were collected, of which 6882 were unique, with R_{int} = 0.0278. Final R_1 (wR_2) = 0. 059 (0.170) with GOF = 1.06.

3 was synthesised by combining 30 mg $Ni(NO_3)_2{\cdot}6H_2O$, 11 mg 2,6-naphthalenedicarboxylic acid (NDC), and 11 mg DPNDI, and 2 mL of DMF in a sealed scintillation vial. The mixture was heated in an oven at 100°C for three days and yielded colourless, plate-shaped crystals. (yield, 11 mg, 16%). FT-IR (ATR, cm^{-1}): 3081w, 3052w, 2894w, 1714m, 1658m, 1650m, 1605m, 1574m, 1493m, 1410s, 1390s, 1344s, 1248s, 1197m, 1147m, 1097m, 1065m, 1025m, 984m, 921, 870m, 830m, 789s, 764s, 754m, 716m, 664m, 640s, 579m, 532m, 473m, 426m.

Crystal data for **3**: $C_{48}H_{57}N_{11}NiO_{15}$. Triclinic, space group *P*-1, a = 11.1115(7), b = 12.5077(8), c = 16.1965(4) Å, α = 85.612(3), β = 89.685(3), γ = 64.385(6)°, V = 2022.9(2) Å^3, Z = 2, D_{calc} = 1.784 g cm^{-3}, μ = 1.540 mm^{-1}, F(000) = 1140. A total of 14755 reflections were collected, of which 7891 were unique, with R_{int} = 0.0508. Final R_1 (wR_2) = 0.054 (0.149) with GOF = 1.03.

Supporting Information

CCDC-1493815 (**1**), CCDC-1493816 (**2**), CCDC-1493817 (**3**) contain the supplementary crystallographic data for this paper. These data can be obtained free of charge from the Cambridge Crystallographic Data Centre via www.ccdc.cam.ac.uk/data_request/cif.

Acknowledgments

We thank the Leverhulme Trust (RPG-2014-317) for support. NRC gratefully acknowledges receipt of a Royal Society Wolfson Merit Award.

References

1. H. Furukawa, K.E. Cordova, M. O'Keeffe and O. M. Yaghi, *Science*, 2013, **341**, 1230444.

2. R. Ricco, C. R. Pfeiffer, K. Sumida, C. J. Sumby, P. Falcaro, S. Furukawa, N.R. Champness and C.J. Doonan, *CrystEngComm*, 2016, **18**, 6532–6542.

3. K. Sumida, D.L Rogow, J. A. Mason, T. M. McDonald, E. D. Bloch, Z. R. Herm, T-H. Bae and J.R. Long, *Chem. Rev.*, 2012, **112**, 724–781.

4. F-K. Shieh, S-C. Wang, C-I. Yen, C-C. Wu, S. Dutta, L-Y. Chou, J. V. Morabito, P. Hu, M-H. Hsu, K. C-W. Wu and C-K. Tsung, *J. Am. Chem. Soc.*, 2015, **137**, 4276–4279.

5. F. Lyu, Y. Zhang, R. N. Zare, J. Ge and Z. Liu, *Nano Lett.*, 2014, **14**, 5761–5765.

6. K. Liang, R. Ricco, C. M. Doherty, M. J. Styles, S. Bell, N. Kirby, S. Mudie, D. Haylock, A. J. Hill, C. J. Doonan and P. Falcaro, P. *Nat. Commun.*, 2015, *6*, 7240.

7. L. Sun, M.G. Campbell and M. Dinca, *Angew. Chem. Int. Ed*. 2016, *55* ,3566 –3579

8. Y. Inokuma, S. Yoshioka, J. Ariyoshi, T. Arai, Y. Hitora, K. Takada, S. Matsunaga, K. Rissanen and M. Fujita, *Nature*, 2013, **495**, 461-466.

9. W. M. Bloch, N. R. Champness and C.J. Doonan, *Angew. Chem. Int. Ed*., 2015, **54**, 12860-12867.

10. S.V. Bhosale, C. H. Jani and S. J. Langford, *Chem. Soc. Rev.*, 2008, **37**, 331-342.

11. K. AlKaabi, C.R. Wade, M. Dincă, *Chem,* 2016, **1**, 264-272.

12. N. Sikdar, K. Jayaramulu, V. Kiran, K. V. Rao, S. Sampath, S.J. George, T.K. Maji, *Chem. Eur. J*. 2015, **21**, 11701-11706.

13. L. Han, L-P. Xu, L. Qin, W-N. Zhao, X-Z. Yan and L. Yu, *Cryst. Growth Des*. 2013, **13**, 4260-4267.

14. Y. Takashima, S. Furukawa and S. Kitagawa, *CrystEngComm* 2011, **13**, 3360-3363.

15. O.K. Farha, C.D. Malliakas, M.G. Kanatzidis and J.T. Hupp, *J. Am. Chem. Soc*. 2010, **132**, 950-952.

16. H. Chung, P.M. Barron, R.W. Novotny, H-T. Son, C. Hu and W. Choe, *Cryst. Growth Des.* 2009, **9**, 3327-3332.

17. C.F. Leong, B. Chan, T. B. Faust and D. M. D'Alessandro, *Chem. Sci*., 2014, **5**, 4724-4728.

18. J-J. Liu, Y. Chen, M-J. Lin, C-C. Huang and W-X. Dai, *Dalton Trans*. 2016, **45**, 6339-6342.

19. Z. Guo, D.K. Panda, K. Maity, D. Lindsey, T.G. Parker, T. E. Albrecht-Schmitt, J.L. Barreda-Esparza, P. Xiong, W. Zhou and S. Saha, *J. Mater. Chem. C*, 2016, **4**, 894-899.

20. J-J. Liu, Y-J. Hong, Y-F. Guan, M-J. Lin, C-C. Huang and W-X. Dai, *Dalton Trans*., 2015, ***44***, 653-658.

21. J-J. Liu, Y. Wang, Y-J. Hong, M-J. Lin, C-C. Huang and W-X. Dai, *Dalton Trans*., 2014, **43**, 17908-17911.

22. S.T. Madrahimov, T.A. Atesin, O. Karagiaridi, A.A. Sarjeant, O.K. Farha, J.T. Hupp and S.T. Nguyen, *Cryst. Growth Des*. 2014, **14**, 6320-6324.

23. N.A. Vermeulen, O. Karagiaridi, A.A. Sarjeant, C.L. Stern, J.T. Hupp, O.K. Farha and J.F. Stoddart, *J. Am. Chem. Soc*. 2013, **135**, 14916-14919.

24. M-H. Xie, X-L. Yang, Y. He, J. Zhang, B. Chen and C-D. Wu, *Chem. Eur. J*. 2013, **19**, 14316-14321.

25. O. Karagiaridi, W. Bury, E. Tylianakis, A.A. Sarjeant, J.T. Hupp and O.K. Farha, *Chem. Mater.* 2013, **25**, 3499-3503.

26. A. Mitra, C.T. Hubley, D.K. Panda, R.J. Clark and S. Saha, *Chem. Commun*. 2013, **49**, 6629-6631.

27. Q. Yang, L. Huang, M. Zhang, Y. Li, H. Zheng and Q. Lu, *Cryst. Growth Des*. 2013, **13**, 440-445.

28. B.J. Burnett, and W. Choe, *CrystEngComm* 2012, **14**, 6129-6131.

29. K. Hirai, H. Uehara, S. Kitagawa and S. Furukawa, *Dalton Trans*. 2012, **41**, 3924-3927.

30. Y. Takashima, V.M. Martinez, S. Furukawa, M. Kondo, S. Shimomura, H. Uehara, M. Nakahama, K. Sugimoto and S. Kitagawa, *Nat. Commun*. 2011, **2**, 168.

31. K.L. Mulfort, O.K. Farha, C.D. Malliakas, M.G. Kanatzidis, and J.T. Hupp, *Chem. Eur. J.* 2010, **16**, 276-281.

32. A.P. Nelson, D.A. Parrish, L.R. Cambrea, L.C. Baldwin, N.J. Trivedi, K.L. Mulfort, O.K. Farha, and J.T. Hupp, *Cryst. Growth Des*. 2009, **9**, 4588-4591.

33. H. Chun, D.N. Dybtsev, H. Kim and K. Kim, *Chem. Eur. J.*, 2005, **11**, 3521-3529.

34. M. Pan, X-M. Lin, G-B. Li and C.-Y. Su, *Coord. Chem. Rev.*, 2011, **255**, 1921-1936.

35. B-Q. Ma, K.L. Mulfort and J.T. Hupp, *Inorg. Chem*. 2005, **44**, 4912-4914.

36. S.R. Batten, N.R. Champness, X-M. Chen, J. Garcia-Martinez, S. Kitagawa, L. Öhrström, M. O'Keeffe, M.P. Suh and J. Reedijk, *Pure Appl. Chem*., 2013, **85**, 1715-1724.

37. X. Fang, X. Yuan, Y-B. Song, J-D. Wang and M-J.; Lin, *CrystEngComm*, 2014, **16**, 9090-9095.

38. A. L. Spek, *J. Appl. Crystallogr.*, 2003, 7-13.

39. J-Z. Liao, X-J. Dui, H-L. Zhang, X-Y. Wu and C-Z. Lu, *CrystEngComm*, 2014, **16**, 10530-10533.

40. CrysalisPro, Oxford Diffraction Ltd.

41. G.M. Sheldrick, *Acta Cryst.,* 2008, **A64**, 112-122.

Graphical Abstract

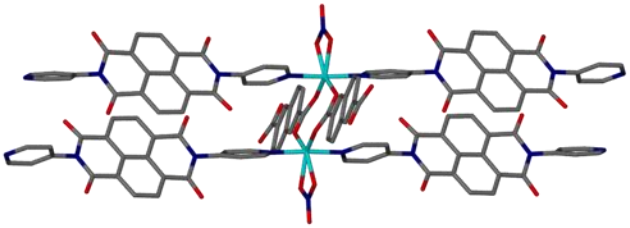

One coordination polymer and two MOFs are created by reacting $Ni(NO_3)_2 \cdot 6H_2O$ with various carboxylic acids. Discussed are the resulting similarities and differences in intermolecular interactions, metal coordination, and cavity dimensions.